Effects of urban morphology on microclimate parameters in an urban university campus.

ZAKI, S.A., OTHMAN, N.E., SYAHIDAH, S.W., YAKUB, F., MUHAMMAD-SUKKI, F., ARDILA-REY, J.A., SHAHIDAN, M.F. and MOHD SAUDI, A.S.

2020

sustainability

MDPI

Article

Effects of Urban Morphology on Microclimate Parameters in an Urban University Campus

Sheikh Ahmad Zaki [1,*], Nurnida Elmira Othman [1,2], Siti Wan Syahidah [1], Fitri Yakub [1], Firdaus Muhammad-Sukki [3], Jorge Alfredo Ardila-Rey [4], Mohd Fairuz Shahidan [5] and Ahmad Shakir Mohd Saudi [6]

1 Malaysia-Japan International Institute of Technology, Universiti Teknologi Malaysia, Jalan Semarak, Kuala Lumpur 54100, Malaysia; elmira5212@gmail.com (N.E.O.); sitiwansyahidah@gmail.com (S.W.S.); mfitri.kl@utm.my (F.Y.)
2 Faculty of Mechanical Engineering, Universiti Teknologi MARA, Shah Alam 40450, Selangor, Malaysia
3 School of Engineering, Robert Gordon University, Garthdee Road, Aberdeen AB10 7GJ, Scotland, UK; f.b.muhammad-sukki@rgu.ac.uk
4 Department of Electrical Engineering, Universidad Técnica Federico Santa María, Santiago de Chile 8940000, Chile; jorge.ardila@usm.cl
5 Faculty of Design and Architecture, Universiti Putra Malaysia, Serdang 43400, Selangor, Malaysia; mohdfairuz@upm.edu.my
6 Environmental Health Research Cluster, Environmental Healthcare Section, Institute of Medical Science Technology, Universiti Kuala Lumpur, Kajang 43000, Malaysia; ahmadshakir@unikl.edu.my
* Correspondence: sheikh.kl@utm.my

Received: 27 February 2020; Accepted: 2 April 2020; Published: 8 April 2020

Abstract: This study investigated the effects of urban morphology on microclimate parameters in an urban university campus in Malaysia. Outdoor air temperatures (T_{out}) were recorded at eight different locations inside the campus for seven days. The study used three urban morphological parameters such as green cover ratio, height-to-width (H/W) ratio, and sky view factor (SVF). The relationship between urban morphological parameters and T_{out} obtained from in situ measurements was investigated. The results showed that, at a dense green cover ratio of 22% in a 7833 m^2 area where the H/W ratio was 0.2, T_{out} was reduced by about 1% due to a long building shadow cover (12 h) and a high range of SVF (from 0.61 to 0.68). The use of geographic information system (GIS) to generate the spatial data of Universiti Teknologi Malaysia Kuala Lumpur Campus (UTMKL), morphological features and in situ T_{out} distributions provided useful information of T_{out} variations, and proved the applicability of GIS as a useful tool in smart city urban planning.

Keywords: urban microclimate; urban morphology; GIS; field measurement; university campus; thermal environment; air temperature; green cover ratio

1. Introduction

Urban greenery is an important element to solve the issues of increased urban temperature caused by the development of built-up environment. At night, vegetation produces thermal heat flux and latent heat flux from solar energy received during the daytime. In this regard, the temperature around the greenery zone is lower in comparison to the area with concrete surfaces and built-up features [1,2]. According to Lowry [3], the presence of trees results in temperature reduction through the process of evapotranspiration, where a dense cluster of six trees induced the cooling effect of 0.3 K/h at noon, with an estimated average of 70 W/m of leaf transpiration. In Tel Aviv, Israel, the cooling effect of 1 K/h is observed at the overwhelming traffic zone with the presence of street trees [4].

The parameters used by previous researchers to quantify the presence of greenery include the green cover ratio and the green plot ratio. The green cover ratio refers to the ratio of the total green area to the total ground cover at a site [4,5]. The coverage of green areas such as grass, shrubs, or trees within a radius of 20 meters is used to define the green cover ratio [5]. Meanwhile, the green plot ratio is measured by considering the leaf mass density such as the leaf area index (LAI) [6].

The studies on the presence of urban greenery can be generally divided into three mode categories, namely application of remote sensing at a large scale (macro scale), field measurement at microscale, and numerical simulation at mesoscale and microscale. The application of remote sensing technology to investigate the effect of green area uses meteorological data and satellite images. Saito [7] evaluated the relationship between meteorological components and green tabulation in Kumamoto City in Japan and inferred that the air temperature variation was firmly identified with the dissemination of greenery in the city.

In addition, field measurement is carried out at microscale, which means it is typically restricted to a specific green area. Jauregui [8] examined that the ambient air temperature in a large urban park in Mexico City was lowered by 2°C to 3°C in comparison to the area made up of built-up features. The temperature reduction was observed within 2 km from the measurement area. Sonne and Vieria [9] conducted measurements at three sites in Melbourne and Florida for over one year, indicating that the forested national park had lower temperature than that of the residential development area. This is due to the extensive presence of tall canopy trees in the national park, providing direct shade from sun radiation and lowering the ambient air temperature during the day. Yang et al. [10] had conducted the field measurement and questionnaire survey to examine relationship of microclimate environments, park use, and human behavioral patterns in the urban area of Umeå, Sweden, which is under subarctic climate. They found that the local residents of Umeå, who expose themselves to a wider climate, are more adapted to subarctic climate than non-local people.

The third mode category, numerical simulation, which is applicable at mesoscale (the intermediate scale between the microscale and large scale) and microscale, can be employed particularly to predict thermal exchange within green areas in cities. Avissar [11] examined the potential effect of vegetation on the urban thermal environment by using a mesoscale atmospheric model. It concludes that vegetation is an important element in urban planning such as heating and cooling requirements of buildings, dispersion and concentration of pollutants, and urban weather. Furthermore, Honjo and Takakura [12] used a numerical model to estimate the temperature reduction in the surroundings of green areas. They pointed out that smaller green areas with enough intervals are desirable for effective cooling of surrounding areas. The improvement in microclimate research significantly contributes to urban planning given two components prevailing the urban climate: Built-up morphology and urban shade trees [13]. Vegetation and water accessibility, regardless of climate conditions, play a major role in reducing heat trapped during the daytime and adequately alleviate the nocturnal urban heat island (UHI) effects. Urban communities should create awareness to ensure that climatological aspects are incorporated within urban design in order to provide a superior living and working environment [14].

Furthermore, the presence of green areas can provide cooling effect and reduce the impact of UHI. Wong and Yu [1] found that the correlation between the presence of green areas and temperature decrease is very high. The study conducted a macroscale mobile survey in Singapore to detect the severity of UHI and the potential of cooling effect in green areas. In addition, a study by Oliveira et al. [15] proved that a small green area (0.24 ha) had a lower temperature than the surrounding area, whereby the highest temperature difference observed was 6.9°C and occurred in the hottest month of the year in Lisbon, Portugal. Katayama et al. [16] investigated the influence of the natural covering ratio on air temperature and found that the area with trees, cultivated fields, grassland, and water bodies consequently reduced the temperature by 2.7°C. They also found that the temperature reduction is greater with longer radius. In this regard, the temperature reduction in a certain radius is based on the surface land covered, which does not only involve the green area, but also buildings, surface pavement type, and geometry of the buildings.

Microclimate studies have been extensively explored in developed countries but are still lacking in developing countries. Most developing countries located in the tropical climate zones are experiencing urbanization whereby urban population is expected to continue increasing in the near future due to continuous economic development. Thus, it has an impact on the urban climate conditions such as dispersion of pollutant and pedestrian discomfort. Therefore, urban design and planning should take into account the quantitative assessment of microclimate of a development area.

To address the aforementioned issue, this study evaluated the local outdoor air temperature and greenery condition inside an urban university campus in Kuala Lumpur, Malaysia, based on the in situ field measurement. Additionally, geographic information system (GIS) was used for generating spatial data and outdoor air temperature maps. The rest of the paper is structured as follows. Section 2 presents the details of the field measurement. Section 3 outlines the results and discussion of this study. Lastly, Section 4 summarizes the findings and conclusions achieved.

2. Field Measurement

2.1. Site Description

This study was conducted at Universiti Teknologi Malaysia Kuala Lumpur Campus (UTMKL) that lies at a latitude of 3.17°N and a longitude of 101.72°E. The campus is located at about 4 km from the city center of Kuala Lumpur. The surrounding of the campus represents the topography of a compact urban area as shown in Figure 1.

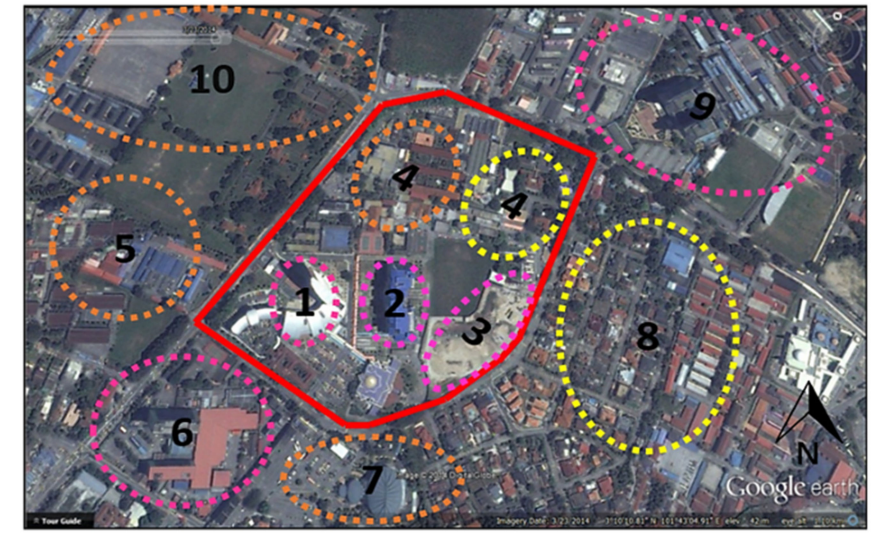

No	Descriptions
1	RAZAK Tower
2	MJIIT Building
3	Construction Area for Student Residential
4	Old Buildings Area in UTMKL
5	Multimedia College
6	Department of Survey and Mapping Malaysia
7	Federal Land and Development Authority Malaysia
8	Residential Area
9	Ministry of Defence
10	Malaysian Police Training Centre

Figure 1. Plan view of the Universiti Teknologi Malaysia Kuala Lumpur Campus (UTMKL) campus and the surrounding area, where numbers 1 to 10 describe the sections outside and inside the campus (Source: Google Earth Image).

UTMKL covers an area of 19.25 hectares. It consists of 78 building blocks, which can be categorized as low-rise, medium, and high-rise buildings. Assuming that a one-story building is 4 m high, the low-rise buildings stand below 10 m, the medium-rise buildings are between 10 m and 30 m high, and the high-rise buildings are above 30 m high. According to Chow and Roth [17], in Singapore, the high-rise buildings, which are typically flats, are between 35 m and 45 m high. On the other hand, the low-rise buildings are generally two-story and three-story buildings.

The in situ measurement of microclimate conditions in UTMKL was conducted from 8 to 14 April 2015. The average outdoor temperature ranged from 27°C to 31°C, and relative humidity (RH) ranged from 69% to 83% based on data collected from the weather station (WS1) installed in this campus during the period of measurement (Table 1). The data were collected for seven days at a 10-min interval. Any missing data, redundant data, and data errors such as data spike and out-of-range data were filtered out before the data were processed and used for analysis. The redundant data and data errors were removed for a more precise analysis. Then, the data were arranged based on daily and hourly averages. These data characterize the local hot and humid climate throughout the year.

Table 1. Statistical results of outdoor air temperature and relative humidity from the weather station (WS1) during the period of measurement. SD is 'standard deviation', Max is 'maximum', and Min is 'minimum'.

Date	Outdoor Air Temperature (°C)				Relative Humidity (%)			
	Average	SD	Max	Min	Average	SD	Max	Min
8/4/15	30.5	3.24	37.6	26.3	70.1	16.15	89.1	35.1
9/4/15	30.1	3.46	38.2	25.4	68.8	16.08	92.2	38.7
10/4/15	28.5	2.24	34.4	25.1	76.4	11.89	91.8	51.5
11/4/15	28.8	3.83	36.3	23.6	75.3	18.00	98.2	42.2
12/4/15	27.3	3.67	37.2	24.4	82.5	15.23	95.6	46.6
13/4/15	28.9	4.02	36.8	24.0	74.9	18.41	95.9	41.1
14/4/15	29.3	3.43	36.4	24.9	75.7	17.30	95.6	44.8

The monitoring locations for the in situ measurement were selected based on different greenery conditions and urban morphology. Eight measurement locations from points A to H, including three stationary weather stations from points 1 to 3, were distributed throughout the campus. Table 2 displays the description of each measurement location based on the ratio of building to greenery (RBG), sky view factor (SVF), and height-to-width (*H/W*) or aspect ratio.

Table 2. Descriptions of the measurement locations.

Location	Description	RBG	SVF	*H/W*
A	Field	1:1.42	0.75	0.49
B	Construction area	1:0.49	0.79	0.89
C	Main entrance gate	1:4.32	0.61	0.27
D	Tennis court	1:0.34	0.68	0.16
E	Engineering laboratory	1:1.15	0.62	0.20
F	Between two low rise buildings	1:1.01	0.61	0.43
G	Parking area	1:1.04	0.97	0.18
H	Between Razak Tower and MJIIT	1:2.49	0.83	1.26
1	Rooftop MJIIT (Weather station 1)	-	-	-
2	Between field and MJIIT (Weather station 2)	-	-	-
3	Main entrance gate (Weather station 3)	-	-	-

RBG: Ratio of building to greenery, SVF: sky view factor, *H/W*: Height-to-width ratio.

The calculation of SVF, which is based on computer algorithm, requires a three-dimensional surface model of the site where both raster and vector input data can be used. However, most of the

input data is the high-resolution digital surface model (DSM) raster data with attributes of terrain and building. The advantage of this method is that it can be managed easily, although the accuracy of the SVF value relies significantly on the image resolution of the input data. Nowadays, many software products, such as BMSky-View [18] and RayMan [19], are configured with calculation algorithms to calculate SVF using fish-eye photographs. Svensson [20] conducted a field measurement study to obtain SVF by capturing fish-eye photographs at 2 m above the ground and at the ground level. The result showed that the fish-eye photograph captured from the ground level was better, as the degree of explanation was improved by up to 12%.

The photos of the instruments and fish-eye photographs at each monitoring location are shown in Figure 2 The SVF values are lower at slightly shaded locations, i.e., locations C and F (SVF = 0.61) compared to at a free space, i.e., location G (SVF = 0.97); the SVF values are shown in Table 2. In this study, the measurement of SVF was carried out using the digital single lens reflex (DSLR) camera and fish-eye lens with a 180° view to capture fish-eye photographs. Such photographs were captured at every in situ fixed station to determine the sky openness of an area. SVF is scaled from 0, for the area with the highest sky obstruction, to 1 for the area with the lowest sky obstruction, which is basically an open area. The sky obstructions were generally observed from buildings and vegetation. The fish-eye photographs were then imported into the Rayman 1.2 software to be processed in order to calculate the SVF value.

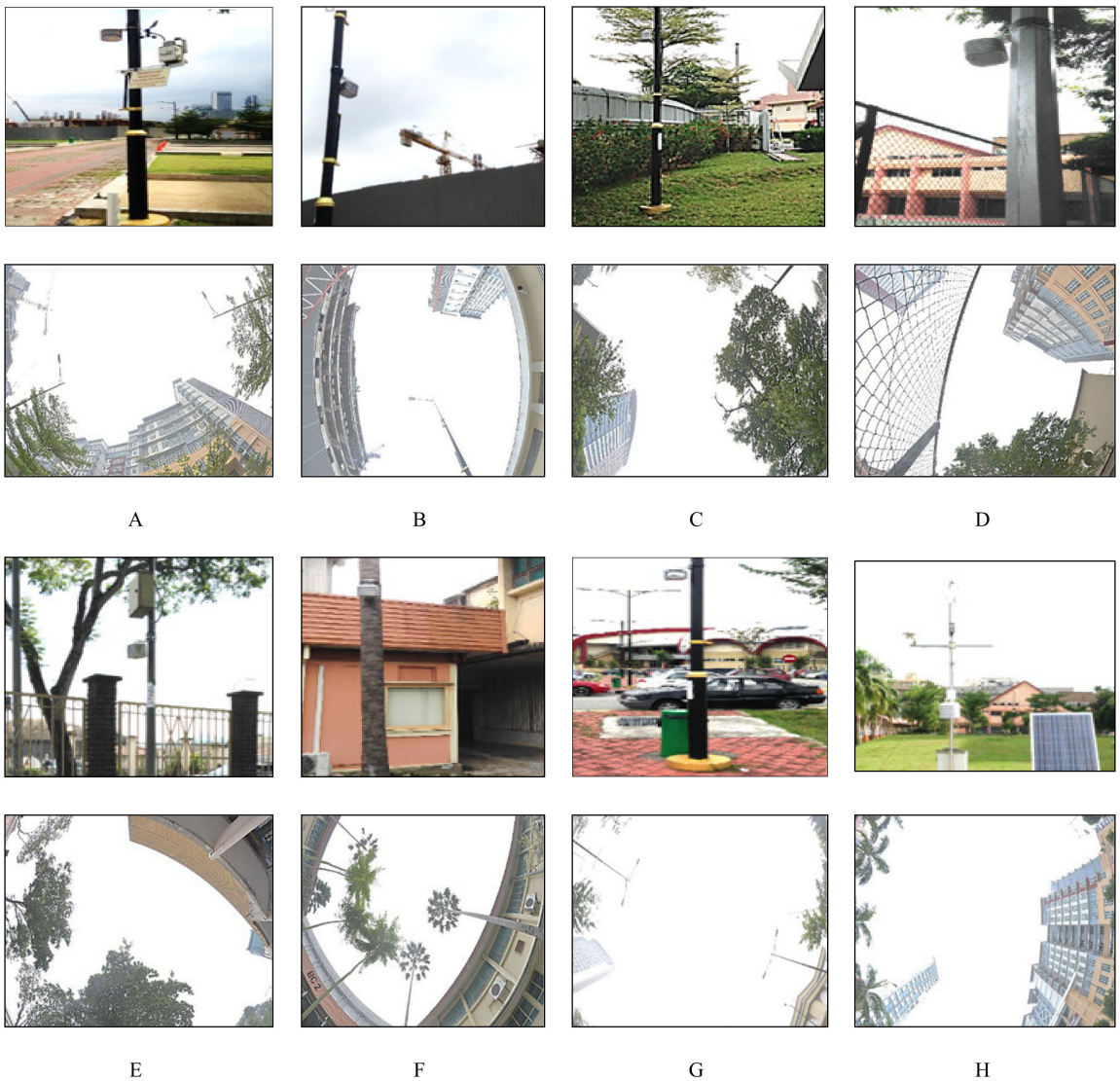

Figure 2. Photos and fish-eye photographs at each monitoring location represented by letters (**A**) to (**H**).

The climatic variables of outdoor air temperature and relative humidity were recorded using the Onset HOBO data loggers at a 10-min interval. The instruments were installed at 3 m above the ground level and attached to the lamp poles to avoid any attempts of vandalism. Furthermore, the distance will allow for more interaction between the ground surface, air, and vegetation. Additionally, 3 weather stations were also installed in this campus. The detailed information of the weather stations can be referred to in the study by Swarno et al. [21] and Othman et al. [22,23]. Table 3 provides a summary of the probing sensors used in this study. All instruments were calibrated and pretested before the field measurement was carried out.

Table 3. Specifications of measurement instruments.

Climatic Variables	Model of Sensor	Measurement Range	Accuracy
Air temperature Relative humidity	Onset HOBO U12-013	−20° to +70 °C 5% to 95%	±0.35 °C ±2.5%

2.2. GIS Application

GIS is a modern application used to store, manage, and geo-spatially analyze various information. This study utilized the GIS technology to manage the microclimatic variables measured at the UTMKL campus in a GIS database. The general workflow of the GIS database development is shown in Figure 3.

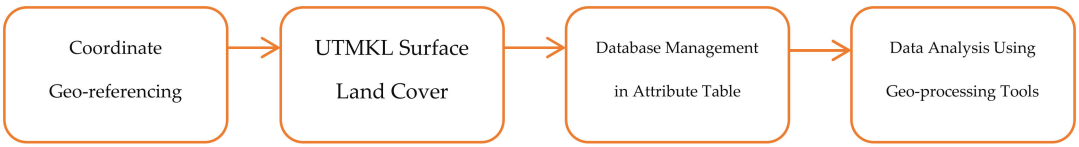

Figure 3. Workflow of the geographic information system (GIS) database development.

The first step for managing the spatial data information was to geo-reference various data sources into one coordinate system. The base map obtained from the Department of Survey and Mapping Malaysia (DSMM) with the projected coordinate system of Geocentric Datum of Malaysia 2000 (GDM2000), Malayan Rectified Skew Orthomorphic (MRSO), were used as a reference to geo-reference other data sources, such as the university campus base map from the UTMKL Estate and Building Department, the WorldView2 satellite image, and Google Earth images into one coordinate system. Next, the land cover data such as greenery area, buildings, construction area, built-up features i.e., parking area, tennis court, and volleyball court, and other features were identified. The land cover data were digitized into vectors to produce a UTMKL map that comprises various land cover features. The information of land covers was classified based on feature class. For every feature class, detailed information such as block's names, locations, and areas were managed. Then, further data analysis on the spatial data characteristics was performed using GIS geo-processing tools.

The GIS application was used for mapping the campus and the distribution of outdoor air temperature. The ArcGIS 10.1 software was used to manage, analyze, and map the data of the campus. The GIS spatial database was used to produce the mapping of greenery and building characteristics. In GIS environment, the analysis of the in situ climatic variables for each station, based on the daily averages of outdoor air temperatures, were inserted into the attribute table. The outdoor air temperatures were interpolated using inverse distance weighted (IDW) interpolation, and raster images were generated. The raster images were overlaid with the UTMKL land covers in order to analyze the areas of high and low temperatures in the campus. The microclimatic mapping included the analysis of greenery and buildings with the outdoor air temperature variation within the radius of 50 m from observation stations. The distribution of outdoor air temperatures was observed based on the GIS air temperature interpolation mapping.

2.3. Greenery Area

The greenery area within UTMKL was identified based on the vector digitization process in the spatial data management stage. The green area attributes such as location, area, and greenery or vegetation type were filled in the database. Types of green areas were classified as grass or shrubs, trees, and park. The green areas were then categorized as open spaces with less greenery, moderate greenery, or dense greenery, as mentioned by Wong and Jusuf [2]. In addition, the green cover ratio was determined by dividing the total green area with the total area of UTMKL. Figure 4 displays the GIS mapping of three types of greenery in the campus, differentiated by colors and textures. The dominant greenery type was grass or shrubs covering 19.5% of the total campus area, followed by trees with 7.7%, and park with only 1.0%.

Figure 4. GIS campus map of greenery types in UTMKL (grass or shrubs, trees, and park).

2.4. Urban Morphology

The parameters of urban morphology include building height, *H/W* ratio, and sky view factor (SVF). In an urban area, building height heterogeneity influences thermal exchange in regard to microclimatic elements i.e., solar radiation and wind flow, and both influence the increase and decrease of urban temperature [24–29]. In addition, the *H/W* ratio is important for determining the inbound shortwave radiation and outbound long-wave radiation for a comfortable urban environment, as well as mitigating the effect of UHI [30–32]. Moreover, sky openness in an urban area is often obstructed by buildings and trees. In this regard, the SVF value decreases due to obstruction from buildings and trees that prevent the net incoming shortwave radiation.

According to Burian [33], buildings are categorized based on height, namely low-rise (0 to 10 m), medium-rise (10 to 30 m), and high-rise (above 30 m). The method used to measure the building height was the three-shot technique. First, the laser rangefinder was aimed straight to the line of sight of the building to measure the slope distance, d. Then, the laser rangefinder was aimed to the bottom of the building, and then to the highest point of the building, to measure the slope angles, θ_2 and θ_1. This

enabled the instrument to automatically calculate and display the height of building, H. The building height was calculated using the equations as follows:

$$a = c \sin \theta_1, \quad (1)$$

$$b = e \sin \theta_2, \quad (2)$$

$$H = a + b, \quad (3)$$

where a is the distance from the horizontal point to the peak of the building, b is the distance from the horizontal point to the base of the building, c is the slope distance from the instrument to the peak of the building, and e is the slope distance from the instrument to the base of the building. Building height, H is the sum of a and b. The height-to-width (H/W) ratio was calculated by the average of two building heights divided by the width between the two buildings. The SVF values were calculated based on the fisheye photograph imported into RayMan 1.2 Software. Figure 5 shows the GIS campus map of building characteristics and H/W ratio. The figure illustrates that low-rise and medium-rise buildings are dominant in this campus. The H/W values at most of the locations in the campus are less than 1.0.

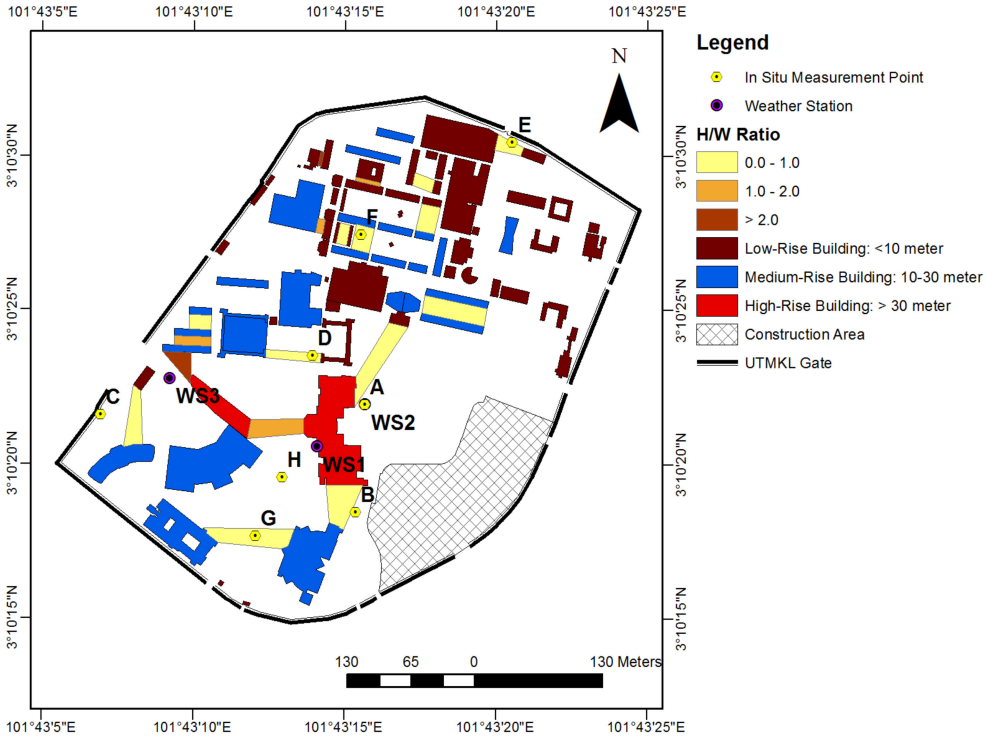

Figure 5. Campus map of building characteristics and H/W ratio.

3. Results and Discussion

3.1. In Situ Measurement Result

The hourly average of outdoor air temperature, T_{out} obtained at different monitoring stations was compared among the eight measurement points, as shown in Figure 6 (for two measurement dates, 8 and 9 April 2015). The highest ambient temperatures were recorded during the daytime at two locations, WS1 and WS3, since there were no obstacles shading the sun radiation. On the other hand, the lowest temperature during the daytime was observed at the monitoring location G due to shading effect by trees and buildings. The inverse condition of temperature at night was observed at all locations. Based on the graph, the average hourly T_{out} was the highest from 12:00 pm to 16:00 pm, while at night, the hourly average of T_{out} was the lowest from 12:00 am to 6:00 am. The highest hourly

average T_{out}, 36.7°C was observed at 16:00 pm on 8 April 2015, while the lowest hourly average of T_{out}, 24.0 °C was observed at 21:00 pm on 11 April 2015. In general, the hourly average of T_{out} was primarily influenced by the weather conditions of rainfall (RF). During the highest hourly average of T_{out}, there was no occurrence of RF throughout the day. However, during the lowest hourly average of T_{out}, a heavy rainfall of 3.2 mm was recorded from 20:00 pm to 21:00 pm.

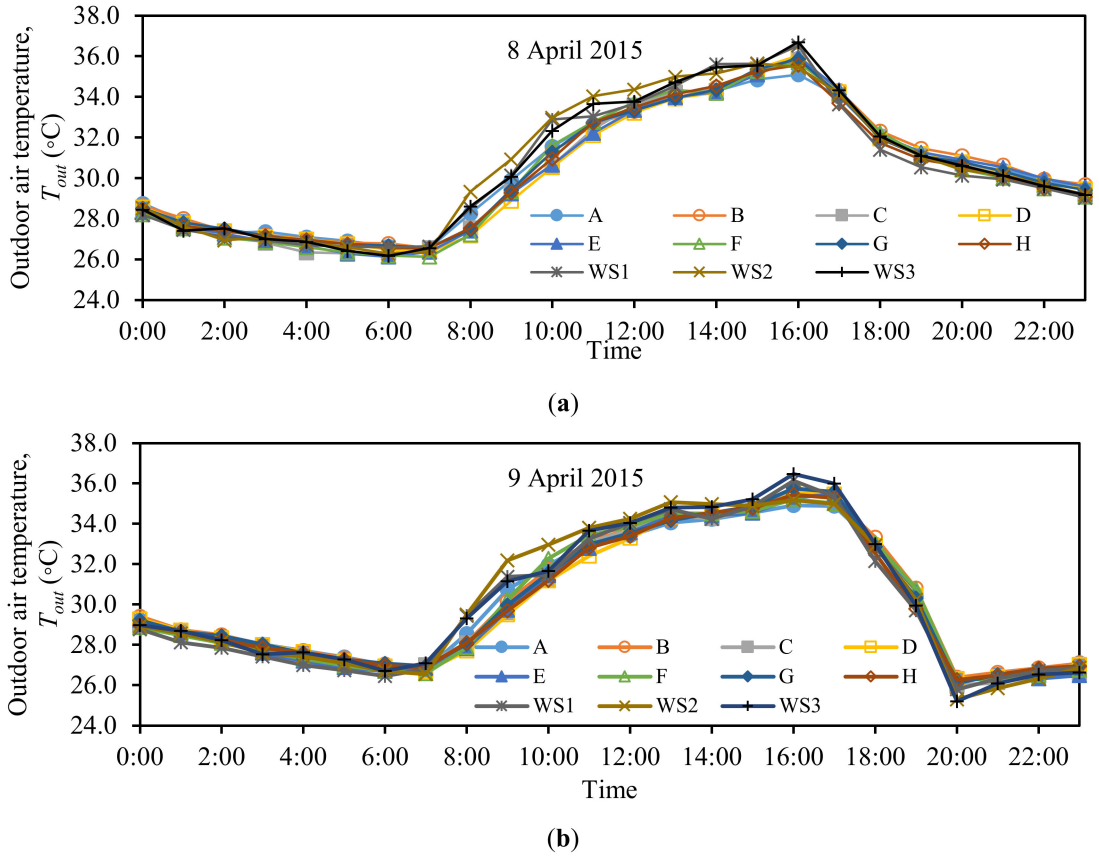

Figure 6. Hourly average outdoor air temperature at eight in situ measurement points and three weather stations, for measurements performed on (**a**) 8 April and (**b**) 9 April 2015.

Table 4 shows the daily average T_{out} and relative humidity (RH) measurements for seven days. The highest daily average of T_{out} was observed on 8 April 2015 and the lowest was on 12 April 2015. The highest and lowest daily averages of T_{out} were associated with the weather conditions of that particular day such as rainfall (RF). On the day with no RF, which was 8 April 2015, the highest daily average of T_{out} was observed, while on 12 April 2015, the total RF of 0.8 mm had lowered the daily average of T_{out}. Figure 7 shows the daily average, maximum, and minimum T_{out}, and RH during the in situ data collections.

Table 4. Statistical values of outdoor air temperature, T_{out} and *RH*.

Date	Outdoor Air Temperature (°C)				Relative Humidity (%)			
	Average	SD	Max	Min	Average	SD	Max	Min
8/4/2015	30.4	2.81	35.2	26.3	67.6	14.68	84.5	37.4
9/4/2015	30.2	3.09	35.2	26.2	65.8	14.95	88.6	38.9
10/4/2015	28.4	2.00	33.1	25.9	75.3	11.62	90.7	53.4
11/4/2015	28.8	3.41	34.7	24.2	73.0	16.35	93.0	44.2
12/4/2015	27.3	2.97	34.4	24.9	81.0	12.97	92.3	49.8
13/4/2015	28.8	3.59	35.0	24.5	73.1	17.09	92.3	41.3
14/4/2015	29.1	2.88	34.2	25.6	74.4	15.70	91.4	47.2

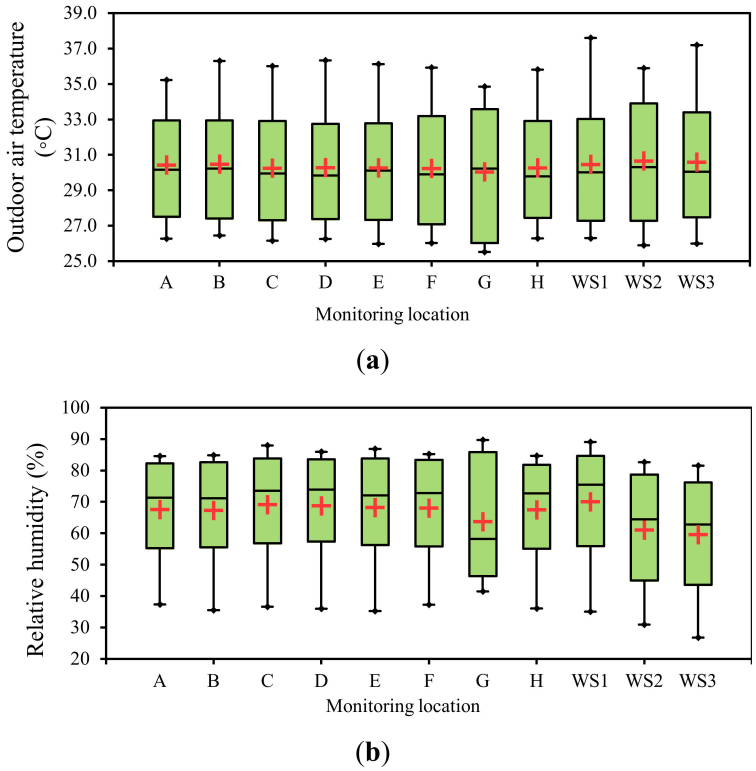

Figure 7. Outdoor air temperature (T_{out}) (**a**) and relative humidity (RH) (**b**) in UTMKL.

3.2. GIS Mapping of Air Temperature

The data of air temperature were collected from 8 April 2015 to 14 April 2015 at eight locations of the in situ point measurement. The additional data from WS1 and WS3 were also used where WS1 was primarily assigned as the reference station. Figure 8 shows the daily air temperature average at eight in situ measurement points from 8 April 2015 to 14 April 2015. The daily air temperature average of 8 April 2015 from all eight measurement points was the highest. This was due to no occurrence of rainfall on that day, which caused the average temperature to rise to the maximum compared to the other days. The lowest air temperature average of all measurement points was observed on 12 April 2015. The total rainfall on that day was 0.8 mm, which was the lowest compared to other measurement days. However, the rainfall event which was observed at 15:00 h on 12 April 2015 was the highest RF occurred during the daytime recorded in the entire measurement period.

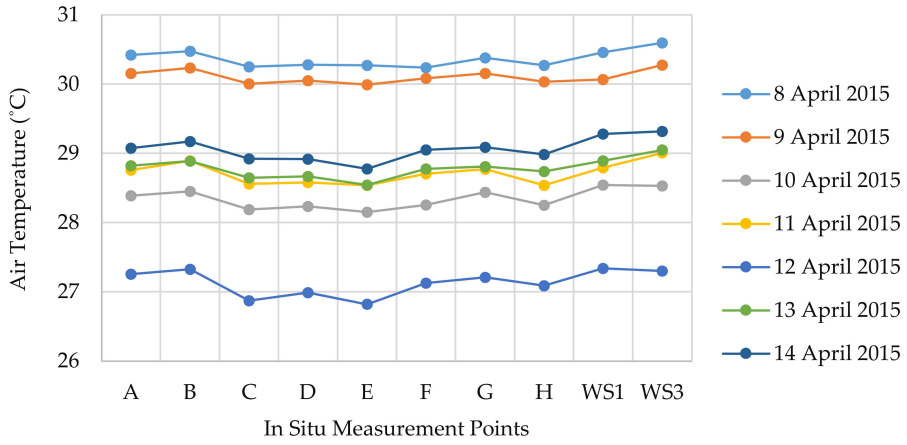

Figure 8. The average daily air temperature data at the eight in situ point measurements, WS1 and WS3.

Figures 9–15 show the daily average air temperature mapped using GIS. The air temperature was interpolated using the inverse distance weighted (IDW) interpolation algorithm [33]; this technique was the most suitable to interpolate the UTMKL daily air temperature distribution since the distance between the two consecutive measurement points was close from one another. The interpolation of climatic variables was visualized in the mapping form and overlaid with the UTMKL land covers for detailed analysis.

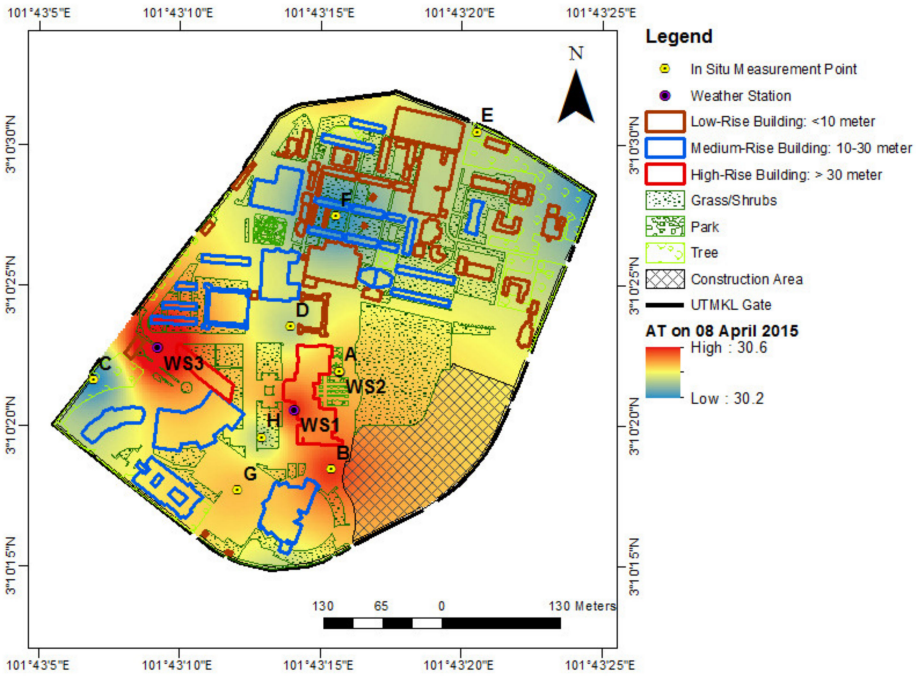

Figure 9. Temperature interpolation in UTMKL dated 8 April 2015.

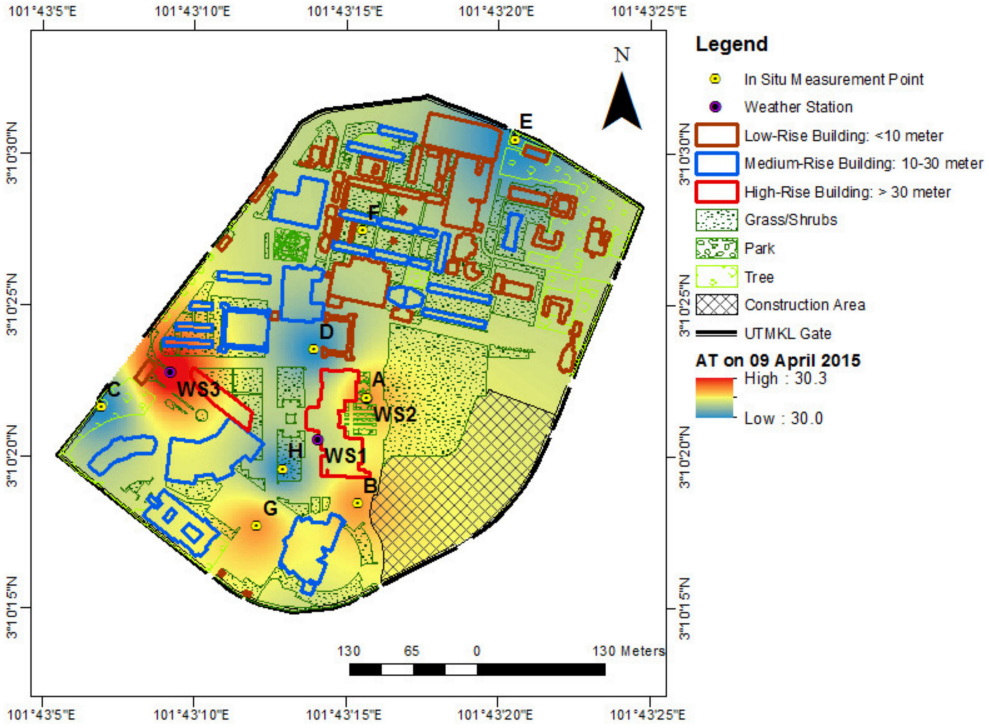

Figure 10. Air temperature interpolation in UTMKL dated 9 April 2015.

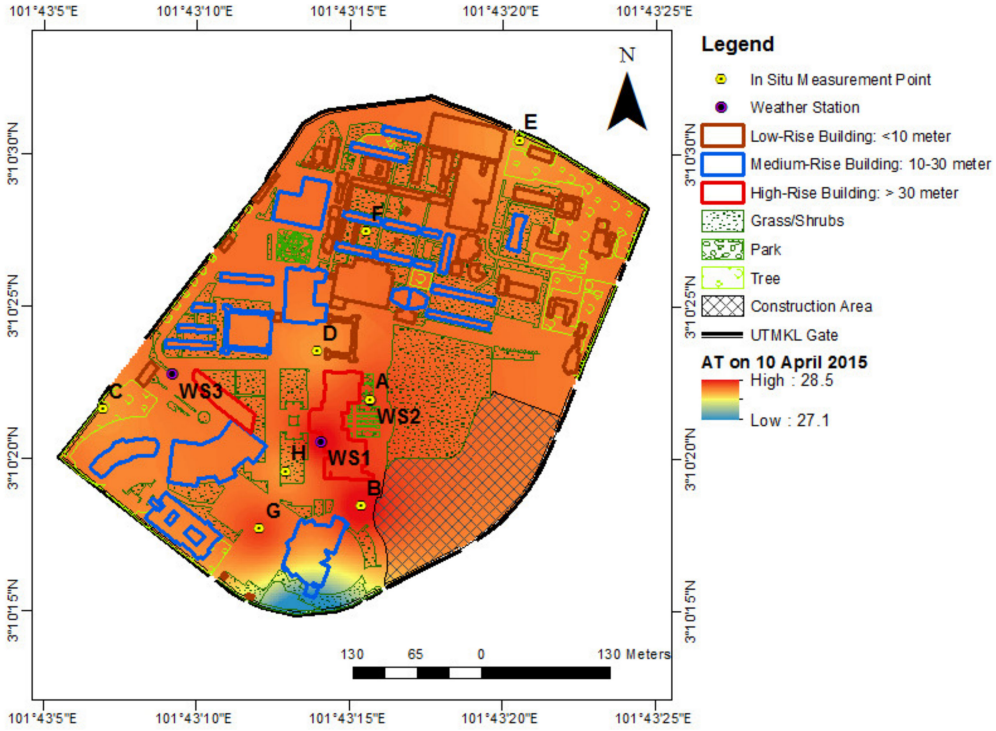

Figure 11. Air temperature interpolation in UTMKL dated 10 April 2015.

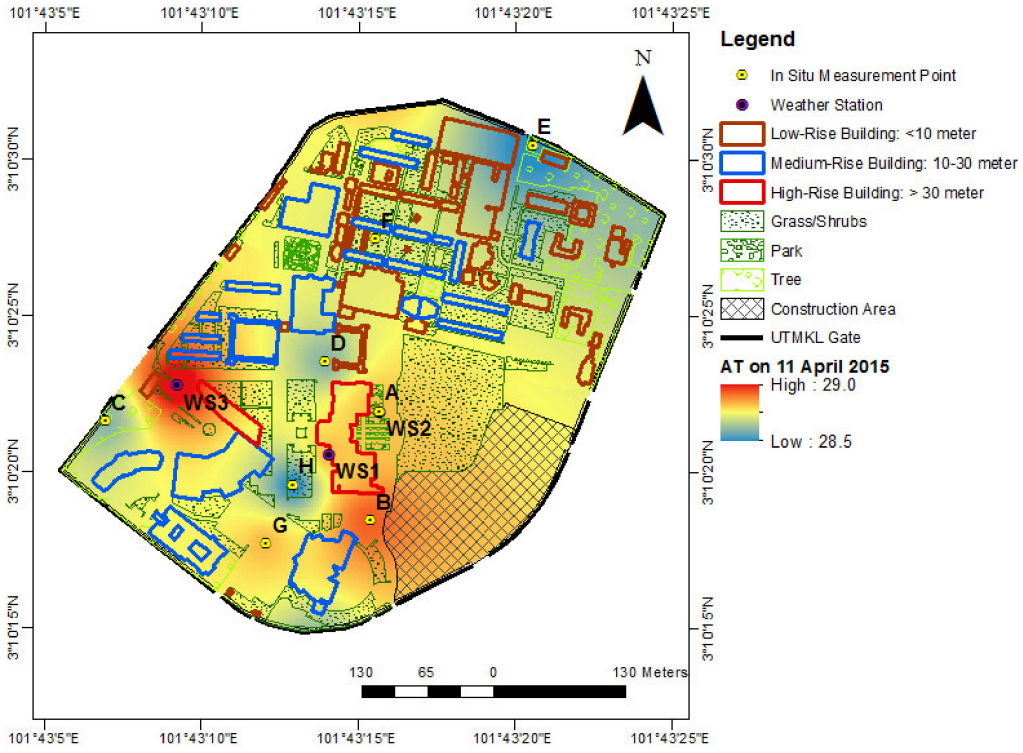

Figure 12. Air temperature interpolation in UTMKL dated 11 April 2015.

Based on Figures 9–15, the daily average air temperatures ranged from 26.8°C to 30.6°C. In these figures, the gradient color marked from blue to red represents the lowest to highest average air temperature. The air temperature interpolation was correlated with the in situ measurement. According to the daily average air temperature interpolation profiles, the red spot that is focused at the weather stations of WS1 and WS2 represents the highest average air temperature in every single day

of measurement. The highest average air temperature condition was most likely the result of highly exposed of radiation where one location is situated at the rooftop of the high-rise building (i.e., WS1) and the other is at the open area with tarmac and the absence of vegetation (i.e., WS2). A similar condition happens in location B where the area was identified as a construction area, which was highly exposed to direct radiation due to the lack of obstruction from building or tree.

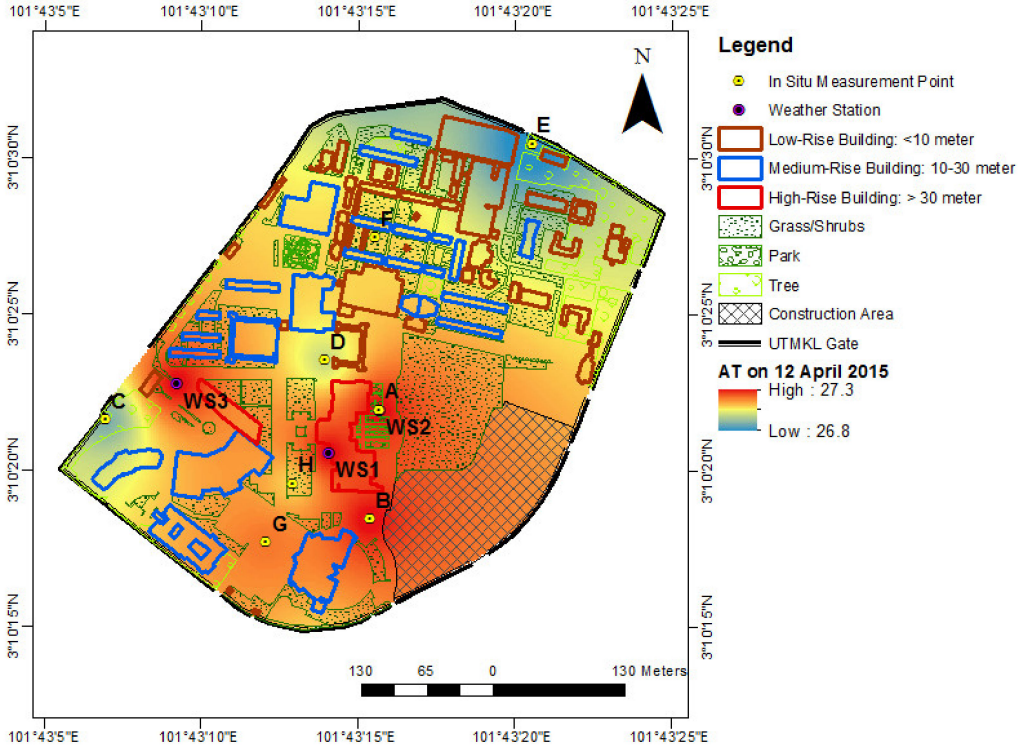

Figure 13. Air temperature interpolation in UTMKL dated 12 April 2015.

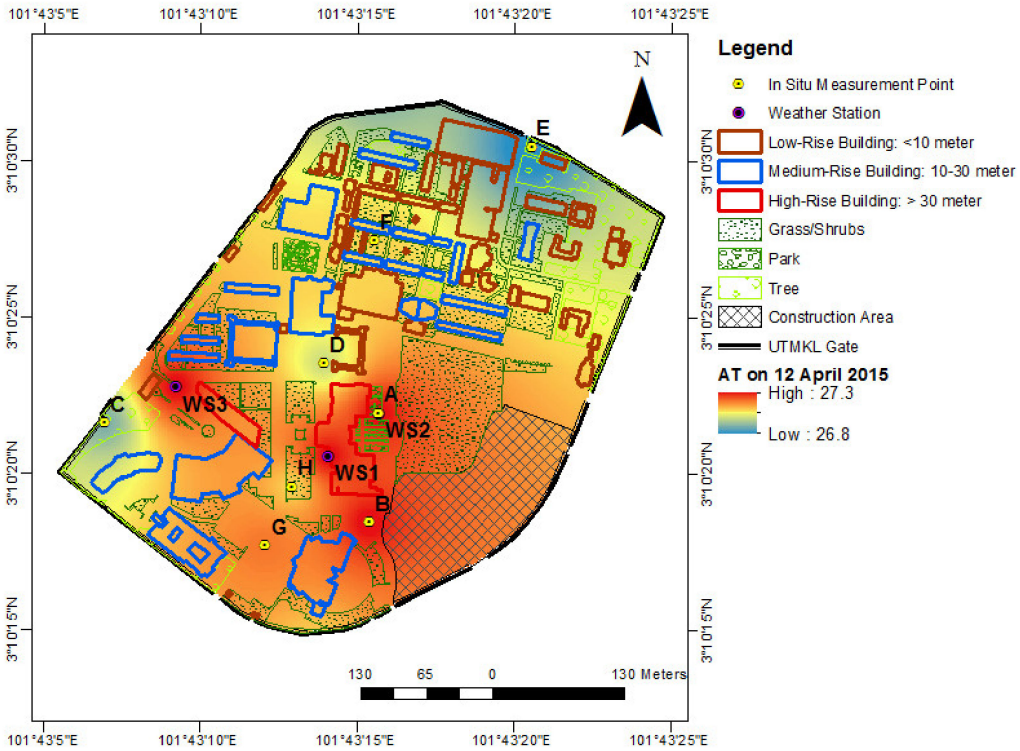

Figure 14. Air temperature interpolation in UTMKL dated 13 April 2015.

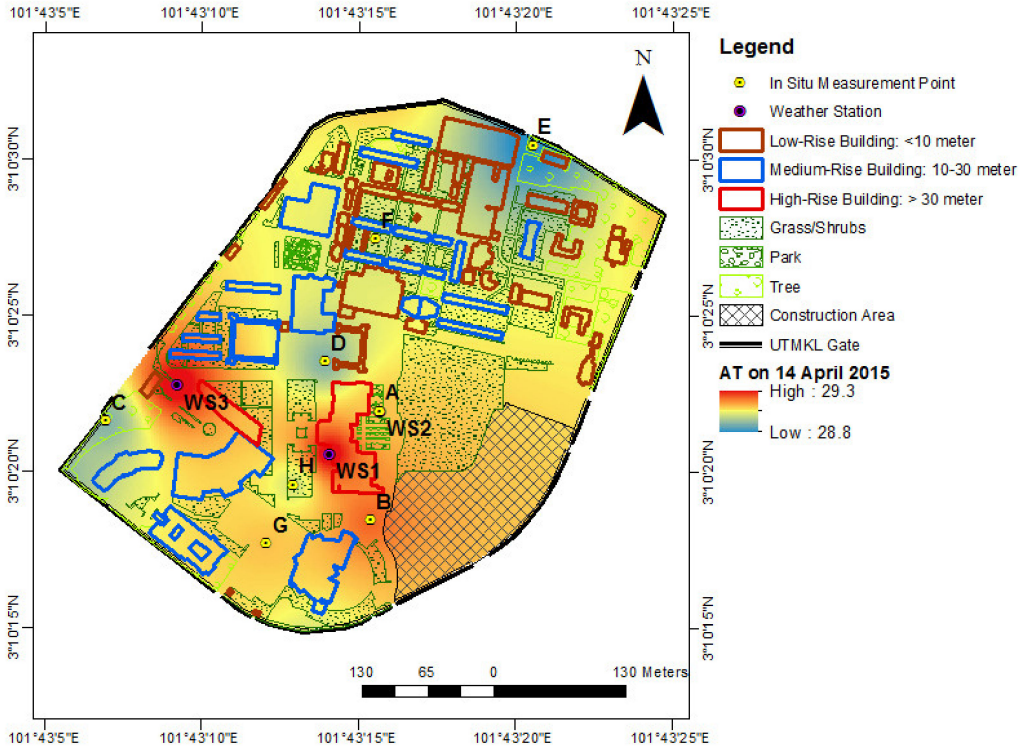

Figure 15. Air temperature interpolation in UTMKL dated 14 April 2015.

Conversely, spots of bluish color representing the lowest average air temperature in every single day of measurement improved the microclimate and kept the area cooler during the daytime. The lowest average air temperature was observed at locations C and E. This was believed to be the result of long exposure to building shadow for almost 12 h, tree shading, and lower range of SVF. These conditions produced a lower air temperature and better ambience of microclimate. Meanwhile, at locations D and H, a similar lower air temperature condition was observed. However, the cooling effect was not sufficient at location D, and this might be due to the use of tarmac as a ground surface material. The low albedo material of tarmac increased the air temperature by reflecting only a small amount of incoming radiation but absorbed most radiation in the absence of the building's shadow. Unlike location D, the improvement was believed to be the result of an increase of grass and shrubs area, which influenced the evapotranspiration rate and consequently reduced the air temperature effectively. Additionally, the average *H*/*W* ratio of the locations that was 0.2 with the dense green cover ratio between 20% and 25% and a high range of SVF led to the reduction of outdoor air temperature by up to 1%.

4. Conclusions

There are two main conclusions based on the research objectives and findings of this study. First, this study performed the microclimatic variables analysis for a complete one-year cycle data of air temperature, relative humidity, solar radiation, and rainfall. The trends of four microclimatic parameters are consistent with those reported in the Malaysian Meteorological Department reports [34–41] on seasonal changes of the country throughout one complete year. The reports showed the fluctuations of the average outdoor air temperature between 24.6°C and 31.3°C, the average relative humidity between 38.3% and 95.8%, while solar radiation peaked at 760 W/m^2. The maximum rainfall occurred during the inter-monsoon seasons in April 2014 (384 mm) and October 2014 (392 mm). In contrast, during the southwest monsoon (from May 2014 to September 2014), total rainfall was relatively lower compared to other seasons, with the lowest total rainfall observed in June 2014 (124 mm). The microclimatic trend

observations for one complete cycle are important to solve any microclimatic issues such as global warming and urban heat island, especially in a tropical hot and humid country like Malaysia.

Secondly, the urban morphological parameters are crucial for assessing the microclimatic changes, in particular, the outdoor air temperature. The urban morphological parameters involved in this study included green area percentage, building shadow, *H/W* ratio, and SVF. Based on these parameters, the outdoor air temperature mapped using GIS was analysed and discussed. The findings explained that the urban morphological parameters such as larger green area, low *H/W* ratio, and high SVF could provide cooling effect to the surrounding area. Combination of building and tree shading and higher green coverage will potentially decrease the effect of excessive radiation and thus improve the outdoor condition significantly.

Thirdly, it can be highlighted that green coverage plays an important role in providing the cooling effect that can effectively lower the ground surface temperature. Green coverage such as grass and shrubs are vital elements to moderate the cooling effect in comparison to low albedo material such as tarmac. It has also been proven that with nearly 25% green coverage area, low *H/W,* and high SVF, the reduction of air temperature by up to 1% can be achieved. In other words, the optimum cooling effect can be achieved by having a larger coverage of the green area, lower *H/W* ratio with dense building condition, and more tree shading coverage. It is also recommended that in the absence of tree planting, grass and shrubs should be located in open spaces to reduce the ground surface temperature. A combination of pavement and grass surface can offer greater cooling effect due to evaporative cooling.

Through these findings, proper campus planning could be suggested in order to support sustainable urban development in line with the Greater Kuala Lumpur Strategic Plan 2020. Moreover, the use of GIS application as a tool for data storage and analysis is an efficient approach to future urban planning and research. The outdoor air temperature mapping and spatial information of urban morphological features such as buildings, vegetation, and other built-up features were managed in a database and visualized in maps. The mapping of both outdoor air temperature and spatial information could improve data interpretation and help urban planners in making decisions regarding the sustainable development process without neglecting the microclimatic elements.

The findings of this study are expected to benefit future studies at local scale. Furthermore, future studies can incorporate additional data collection techniques, such as daily measurement and mobile measurement to visualize both diurnal and nocturnal effects of urban morphological parameters and microclimate variables covering a larger area.

Author Contributions: Conceptualization, S.A.Z.; data curation, S.A.Z. and S.W.S.; formal analysis, S.A.Z. and S.W.S.; funding acquisition, S.A.Z., F.Y., J.A.A.-R., and F.M.-S.; investigation, S.A.Z. and S.W.S.; methodology, S.A.Z.; project administration, S.A.Z.; resources, S.A.Z.; software, S.A.Z.; supervision, S.A.Z. ; validation, S.A.Z. and S.W.S.; visualization, S.A.Z., S.W.S., and F.M.-S.; writing—original draft, S.A.Z., S.W.S., and N.E.O; writing—review and editing, S.A.Z., S.W.S., N.E.O., F.Y., J.A.A.-R., F.M.-S., M.F.S., and A.S.M.S. All authors have read and agreed to the published version of the manuscript.

Funding: This work was supported by Ministry of Education (MOE) through Fundamental Research Grant Scheme [FRGS/1/2019/TK07/UTM/02/5], Universiti Teknologi Malaysia under Matching Grant [Vot 01M89], Agencia Nacional de Investigación y Desarrollo (through the project Fondecyt regular 1200055 and the project Fondef ID19I10165) and project PI_m_19_01 (UTFSM).

Conflicts of Interest: The authors declare no conflict of interest. The funders had no role in the design of the study; in the collection, analyses, or interpretation of data; in the writing of the manuscript, or in the decision to publish the results.

References

1. Wong, N.H.; Yu, C. Study of green areas and urban heat island in a tropical city. *Habitat Int.* **2005**, *29*, 547–558. [CrossRef]
2. Wong, N.H.; Jusuf, S.K. Study on the microclimate condition along a green pedestrian canyon in Singapore. *Archit. Sci. Rev.* **2010**, *53*, 196–212. [CrossRef]

3. Lowry, W.P. Atmospheric Ecology for Designers and Planners. *Landsc. J. Book Rev.* **1990**, *9*, 155–156. [CrossRef]
4. Shashua-Bar, L.; Hoffman, M.E. Vegetation as a climatic component in the design of an urban street. *Energy Build.* **2000**, *31*, 221–235. [CrossRef]
5. Yang, F.; Lau, S.S.Y.; Qian, F. Summertime heat island intensities in three high-rise housing quarters in inner-city Shanghai China: Building layout, density and greenery. *Build. Environ.* **2010**, *45*, 115–134. [CrossRef]
6. Ong, B.L. Green Plot Ratio: An ecological measure for architecture and urban planning. *Landsc. Urban Plan.* **2003**, *63*, 197–211. [CrossRef]
7. Saito, I.; Ishihara, O.; Katayama, T. Study of the effect of green areas on the thermal environment in an urban area. *Energy Build.* **1990**, *15*, 493–498. [CrossRef]
8. Jauregui, E. Influence of a large urban park on temperature and convective precipitation in a tropical city. *Energy Build.* **1990**, *15*, 457–463. [CrossRef]
9. Sonne, J.K.; Vieira, R.K. Cool neighborhoods: The measurement of small scale heat islands. *Proc. Aceee Summer Study Energy Effic. Build.* **2000**, *1*, 1307–1318.
10. Yang, B.; Olofsson, T.; Nair, G.; Kabanshi, A. Outdoor thermal comfort and human behavior pattern under subarctic climate of north Sweden—A pilot study in Umeå. *Sustain. Cities Soc.* **2017**, *28*, 387–397. [CrossRef]
11. Avissar, R. Potential effects of vegetation on the urban thermal environment. *Atmos. Environ.* **1996**, *30*, 437–448. [CrossRef]
12. Honjo, T.; Takakura, T. Simulation of thermal effects of urban green areas on their surrounding areas. *Energy Build.* **1990**, *16*, 443–446. [CrossRef]
13. Shashua-Bar, L.; Tsiros, I.X.; Hoffman, M.E. A modeling study for evaluating passive cooling scenarios in urban streets with trees. Case study: Athens, Greece. *Build. Environ.* **2010**, *45*, 2798–2807. [CrossRef]
14. Roth, M. Review of urban climate research in subtropical regions. *Int. J. Climatol.* **2007**, *27*, 1859–1873. [CrossRef]
15. Oliveira, S.; Andrade, H.; Vaz, T. The cooling effect of green spaces as a contribution to the mitigation of urban heat: A case study in Lisbon. *Build. Environ.* **2011**, *46*, 2186–2194. [CrossRef]
16. Katayama, T.; Ishii, A.; Hayashi, T.; Tsutsumi, J. Field surveys on cooling effects of vegetation in an urban area. *J. Therm. Biol.* **1993**, *18*, 571–576. [CrossRef]
17. Chow, W.T.L.; Roth, M. Temporal Dynamics of the Urban Heat Island of Singapore. *Int. J. Climatol.* **2006**, 2243–2260. [CrossRef]
18. Gal, T.; Unger, J. A new software tool for SVF calculations using building and tree-crown databases. *Urban Clim.* **2014**, *10*, 594–606. [CrossRef]
19. Matzarakis, A. RayMan and SkyHelios Model—Two Tools for Urban Climatology. *Fachtag. Des Aussch. Umw. Der Dtsch. Meteorol. Ges.* **2012**, *5*, 1–6.
20. Svensson, M.K. Sky view factor analysis—implications for urban air temperature differences. *Meteorol. Appl.* **2004**, *11*, 201–211. [CrossRef]
21. Aini Swarno, H.; Ahmad Zaki, S.; Yusup, Y.; Sukri Mat Ali, M.; Huda Ahmad, N. Observation of Diurnal Variation of Urban Microclimate in Kuala Lumpur, Malaysia. *Chem. Eng. Trans.* **2017**, *56*, 523–528. [CrossRef]
22. Othman, N.E.; Zaki, S.A.; Ahmad, N.H.; Razak, A.A. In-situ Measurement of Pedestrian Outdoor Thermal Comfort in Universities Campus of Malaysia. *Kne Soc. Sci.* **2019**, 608–621. [CrossRef]
23. Othman, N.E.; Zaki, S.A.; Ahmad, N.H.; Razak, A.A. Outdoor thermal comfort study of an urban university campus in Malaysia. *J. Adv. Res. Fluid Mech. Therm. Sci.* **2019**, *57*, 288–296, ISSN: 22897879.
24. Memon, R.A.; Leung, D.Y.C.; Chunho, L.I.U. A review on the generation, determination and mitigation of urban heat island. *J. Environ. Sci.* **2008**, *20*, 120–128. [CrossRef]
25. Kruger, E.L.; Minella, F.O.; Rasia, F. Impact of urban geometry on outdoor thermal comfort and air quality from field measurements in Curitiba, Brazil. *Build. Environ.* **2011**, *46*, 621–634. [CrossRef]
26. Perini, K.; Magliocco, A. Effects of vegetation, urban density, building height, and atmospheric conditions on local temperatures and thermal comfort. *Urban For. Urban Green.* **2014**, *13*, 495–506. [CrossRef]
27. Sharmin, T.; Steemers, K.; Matzarakis, A. Analysis of microclimatic diversity and outdoor thermal comfort perceptions in the tropical megacity Dhaka, Bangladesh. *Build. Environ.* **2015**, *94*, 734–750. [CrossRef]
28. Oke, T.R. Boundary Layer Climates Second Edition (Book). *RoutledgeTaylor Fr. Group* **1987**. [CrossRef]

29. Giridharan, R.; Ganesan, S.; Lau, S.S. Daytime urban heat island effect in high-rise and high-density residential developments in Hong Kong. *Energy Build.* **2004**, *36*, 525–534. [CrossRef]
30. Xi, T.; Li, Q.; Mochida, A.; Meng, Q. Study on the outdoor thermal environment and thermal comfort around campus clusters in subtropical urban areas. *Build. Environ.* **2012**, *52*, 162–170. [CrossRef]
31. Ahmed, A.Q.; Ossen, D.R.; Jamei, E.; Manaf, N.A.; Said, I.; Ahmad, M.H. Urban surface temperature behaviour and heat island effect in a tropical planned city. *Theor. Appl. Climatol.* **2014**, 1–22. [CrossRef]
32. Giannopoulou, K.; Santamouris, M.; Livada, I.; Georgakis, C.; Caouris, Y. The impact of canyon geometry on intra Urban and Urban: Suburban night temperature differences under warm weather conditions. *Pure Appl. Geophys.* **2010**, *167*, 1433–1449. [CrossRef]
33. Burian, S.J.; Brown, M.J.; Linger, S.P. Morphological Analyses using 3D Building Databases: Los Angeles, California. *Los Alamos Natl. Lab.* **2002**, *74*, 836.
34. Yunus, F.; Jaafar, J.; Mahmod, Z.; Chang, N.K. The influence of air temperature controls in estimation of air temperature over homogeneous terrain. *Appl. Ecol. Environ. Sci.* **2014**, *2*, 141–145. [CrossRef]
35. Malaysia Meteorological Department. *Annual Report 2014*; Malaysia Meteorological Department: Kuala Lumpur, Malaysia, 2014.
36. Malaysia Meteorological Department. *Northeast Monsoon Report 2014*; Malaysia Meteorological Department: Kuala Lumpur, Malaysia, 2014.
37. Malaysia Meteorological Department. *Southwest Monsoon Report 2014*; Malaysia Meteorological Department: Kuala Lumpur, Malaysia, 2014.
38. Malaysia Meteorological Department. *Annual Report 2015*; Malaysia Meteorological Department: Kuala Lumpur, Malaysia, 2015.
39. Malaysia Meteorological Department. Iklim Malaysia. 2017. Available online: http://www.met.gov.my/web/metmalaysia/climate/generalinformation/malaysia (accessed on 6 January 2017).
40. Yip, W.S.; Diong, J.Y.; Chang, N.K.; Mat Adam, M.K.; Fakaruddin, F.J.; Saleh, F.Z.; Abdullah, M.H. *Analysis of the Northeast Monsoon 2014/2015, Petaling Jaya Selangor Malaysia*; Malaysian Meteorolofical Department (MMD) and Ministry of Science, Technology and Innovation (MOSTI): Kuala Lumpur, Malaysia, 2015; pp. 1–34.
41. MMD. Malaysia Meteorological Department. 2016. Available online: http://www.met.gov.my/web/metmalaysia/climate/generalinformation/malaysia (accessed on 16 June 2016).